

Confluence and tight junction dependence of volume regulation in epithelial tissue

Theresa A. Chmiel and Margaret L. Gardel¹*

Institute for Biophysical Dynamics, James Franck Institute, Department of Physics, Pritzker School of Molecular Engineering, University of Chicago, Chicago, IL 60637

ABSTRACT Epithelial cell volume regulation is a key component to tissue stability and dynamics. In particular, how cells respond to osmotic stresses is of significant physiological interest in kidney epithelial tissue. For individual mammalian cells, it is well established that Na-K-2Cl cotransporter (NKCC) channels mediate cell volume homeostasis in response to hyperosmotic stress. However, whether mature epithelium responds similarly is not well known. Here we show that while small colonies of madin darby canine kidney (MDCK) epithelial cells behave similarly to single cells and exhibit volume homeostasis that is dependent on the NKCC channel function, mature epithelial tissue does not. Instead, the cell volume decreases by 33% when confluent monolayers or acini formed from MDCK cells are subjected to hyperosmotic stress. We show that the tight junction protein zonula occludins-1 (ZO-1), and Rho-associated kinase (ROCK) are essential for osmotic regulation of cell volume in mature epithelium. Because these both are known to be essential for tight junction assembly, this strongly suggests a role for tight junctions in changing volume response in mature epithelium. Thus, tight junctions act either directly or indirectly in osmotic pressure response of epithelial tissue to suppress volume homeostasis common to isolated epithelial cells.

Monitoring Editor

Valerie Marie Weaver
University of California,
San Francisco

Received: Mar 2, 2022
Revised: Jun 13, 2022
Accepted: Jun 15, 2022

INTRODUCTION

Epithelial cells actively regulate their volume in response to osmotic gradients through management of ion concentration and cytoskeletal tension (Delpire and Gagnon, 2018). Animal cells lack rigid structures that would help to maintain an osmotic gradient across the plasma membrane, meaning that when osmotic pressure is applied to the membrane, a cell must respond with a sizable deformation to the membrane or risk rupture (Strange, 1993; Hoffmann et al., 2009). It does so primarily by controlling the movement of solutes across the cell membrane through tightly regulated ion channels (Finan and Guilak, 2010). And so, while osmotic stress is a mechanical force on a tissue, how the cells in that tissue respond

physically and the regulatory pathways involved in this response are significantly more complicated.

The pump-leakage model is the basic model that is used to understand regulation of cell volume through ion transport and in response to changes in external or internal osmotic pressure (Strange, 1993). When hypertonic media are introduced, highly membrane-permeable water initially rushes out of the cell, causing the cell to shrink in volume. The cell then reacts by activating a variety of transport channels, and predominantly the Na-K-2Cl cotransporter (NKCC) family, to increase ion concentration in the cytoplasm and restore the osmotic gradient (Haas, 1994; Delpire and Gagnon, 2018). This process to reestablish cell volume after a hyperosmotic shock is known as a regulatory volume increase (RVI).

The response to osmotic gradients in epithelial tissue is not as well understood as in single cells, but presumably involves both cell- and tissue-scale responses. In polarized epithelial tissue, tight junctions assemble at the apical surface and create a barrier to prevent the extracellular flow of osmolytes across the epithelial tissue (Günzel and Yu, 2013; Varadarajan et al., 2021). Tight junctions prevent “leakiness” in epithelial tissue and are designed to act as a barrier between the internal and external cellular environments (Fischbarg, 2010; Tokuda and Yu, 2019). The integrity of the tight junction is critical for proper organ function (Lee et al., 2006; Liu et al., 2012; Lee et al., 2018), and the depletion of either the tight

This article was published online ahead of print in MBoc in Press (<http://www.molbiolcell.org/cgi/doi/10.1091/mbc.E22-03-0073>) on June 22, 2022.

*Address correspondence to: Margaret L. Gardel (gardel@uchicago.edu).

Abbreviations used: MDCK, madin darby canine kidney; NKCC, Na-K-2Cl cotransporter; ROCK, Rho-associated protein kinase; RVI, regulatory volume increase; ZO-1, zonula occludins-1.

© 2022 Chmiel and Gardel. This article is distributed by The American Society for Cell Biology under license from the author(s). Two months after publication it is available to the public under an Attribution-Noncommercial-Share Alike 4.0 International Creative Commons License (<http://creativecommons.org/licenses/by-nc-sa/3.0>).

“ASCB®,” “The American Society for Cell Biology®,” and “Molecular Biology of the Cell®” are registered trademarks of The American Society for Cell Biology.

junction protein zonula occludens-1 (ZO-1; Odenwald *et al.*, 2018) or the cytoskeletal regulator Rho-associated protein kinase (ROCK; Walsh *et al.*, 2001) results in increased tissue permeability. Renal epithelium in particular is consistently exposed to changing osmotic conditions, as solute concentration passing through the kidney is constantly in flux (Beck *et al.*, 1998).

Because the tight junctions regulate osmotic flow across the epithelium, they control the spatial regulation of osmotic stress on the tissue. In addition, polarized renal epithelial tissue confines NKCC1, a member of the NKCC family of ion channels, to the basolateral membrane (Carmosino *et al.*, 2008) and away from any osmotic stresses at the apical surface of the tissue. This functions to create not just an osmotic pressure gradient across a cell's plasma membrane, as we observe in single cells, but a differential pressure gradient across the epithelial tissue, the regulation of and cellular response to which is not well understood.

Here, we examine the mechanics of volume regulation in renal epithelial tissue formed from madin darby canine kidney (MDCK) cells and find both a confluence and a tight junction dependence on the tissue's ability to maintain volume homeostasis under hypertonic conditions. We find that small colonies of epithelial tissue exhibit volume homeostasis in response to hyperosmotic stress, in a mechanism reliant on NKCC channels. However, the volume of cells within mature monolayers and acini is acutely suppressed hours after hypertonic conditions are introduced, indicating inhibition of the process of regulatory volume increase. Disruption of tight junctions in mature monolayers, through either the depletion of ZO-1 or the inhibition of ROCK, recovers volume homeostasis in response to hyperosmotic stress. Based on these findings, we report a role of the tight junctions in qualitatively modifying cell volume regulation in epithelial tissue.

RESULTS

Cell volume in epithelial colonies recovers from hyperosmotic shock via Na-K-2Cl cotransporter-mediated regulatory volume increase

To measure the volume response of renal epithelium to osmotic stress, we plated MDCK-II cells sparsely on glass and allowed them to grow for 24 h, creating small colonies of 4–37 cells, and imaged them fluorescently with the addition of CellMask Orange membrane stain. We exposed these colonies to either isotonic (normal DMEM medium) or hypertonic (an added 200 mM of the synthetic sugar sorbitol) conditions for 3 h and examined whether the colony was able to recover its isotonic volume (Figure 1A), that is, whether the colony was able to undergo RVI and maintain volume homeostasis. We observed that the average colony cell volume after a long-term hypertonic shock is slightly but not significantly reduced compared with the average volume of colonies in isotonic conditions (Figure 1B). In addition, when we examine a colony immediately after the addition of hyperosmotic medium, we see that there is an initial decrease in the average cell volume, followed by almost complete volume recovery consistent with RVI (Figure 1C). In these data, we see a slight increase in the average cell volume of the isotonic/control cells immediately following the addition of new medium. Initial changes in isotonic volume following the agitation of the wash-in can be seen in many of our time-lapse data and indicate that there is a transient effect of agitation that occurs on a much shorter time scale than the observed RVI.

We next wanted to confirm that the volume recovery observed is due to ion channel activity as expected for RVI. MDCK cells express exclusively Na⁺-K⁺-Cl⁻ cotransporter 1 (NKCC1), which has been found to localize basolaterally in epithelial tissue (Mykoniatis *et al.*,

2010; Koumangoye *et al.*, 2018). We treated colonies with 10 μM of bumetanide, a NKCC inhibitor, and saw that volume homeostasis in response to hypertonic conditions is abrogated (Figure 1D). Cell volume is significantly reduced after 3 h of hypertonic conditions in the presence of NKCC inhibitor, compared with that of cells under isotonic conditions (Figure 1E). After 3 h, NKCC inhibition under hyperosmotic conditions resulted in a reduction in average colony cell volume to 74% of isotonic cell volume, while control cells were able to recover to 89% of their initial volume (Figure 1F). This indicates that small colonies of MDCK cells exhibit volume homeostasis mediated by NKCC channels, consistent with a well-established RVI mechanism that maintains volume homeostasis in single cells in response to hyperosmotic stress.

Characterization of monolayer volume and volume variation

To explore changes in cell volume occurring in mature epithelium, we developed protocols to characterize the changes in cell volume. MDCK-II cells are plated densely on glass slides and grown for 48 h with 100% confluency achieved after 24 h, creating a mature epithelial tissue. CellMask Orange membrane dye is added before imaging to clearly outline the apical and basal membranes in monolayers (Figure 2A). This allows us to calculate average monolayer height for a desired field of view in a sample through plotting the average intensity for each slice of our three-dimensional image and fitting the two peaks in intensity, which represent the apical and basal membranes of the sample, to a gaussian (Figure 2B). The difference between these two peaks is the local average height of the monolayer. We then measure the average cross-sectional area and approximate average cell volume in a monolayer as the average cross-sectional area multiplied by the average monolayer height (Figure 2C).

MDCK monolayers exhibit natural variation in both cell density and cell volume (Zehnder *et al.*, 2015) (Figure 2D) and the scale of this variation can be seen within a single 135 × 175 μm² field of view (Figure 2E). We chose this range to average over because the natural variation in local volume is consistent with the average variation in volume between one monolayer and another (Figure 2F), allowing us to treat each field of view's local volume as independent.

Mature epithelial tissue does not recover from a long-term osmotic shock

We next perform iso- and hypertonic experiments on mature epithelium formed by plating MDCK cells at high density onto glass and incubating for 48 h. Under these conditions, tight junctions form in this polarized model epithelial tissue to facilitate well-characterized barrier function (Lee *et al.*, 2006; Fischberg, 2010). Under this condition, the hyperosmotic medium presumably remains confined to the apical cell surface. Upon medium exchange to hypertonic conditions, we discover that the average volume of the cells decreases by 20–35% and does not recover over time, so that the epithelial height and volume remain permanently reduced even after 3 h (Figure 3, A–C).

To determine whether mature epithelial tissue reacts similarly independent of configuration, we performed these experiments in MDCK acini in collagen gel. MDCK acini are confluent cysts that are formed by seeding cells sparsely within collagen gel and incubating for 8 days. Acini are polarized with the apical surface at the inner surface of the cyst known as the lumen and the basal surface facing the external media. Thus, for acini, the basal and basolateral cell surfaces are exposed to the exchanged media and the barrier prevents transport to the apical surface. Similarly to confluent monolayers, the hyperosmotic shock permanently reduces the volume of cells within acini by 34% (Figure 3, D and E).

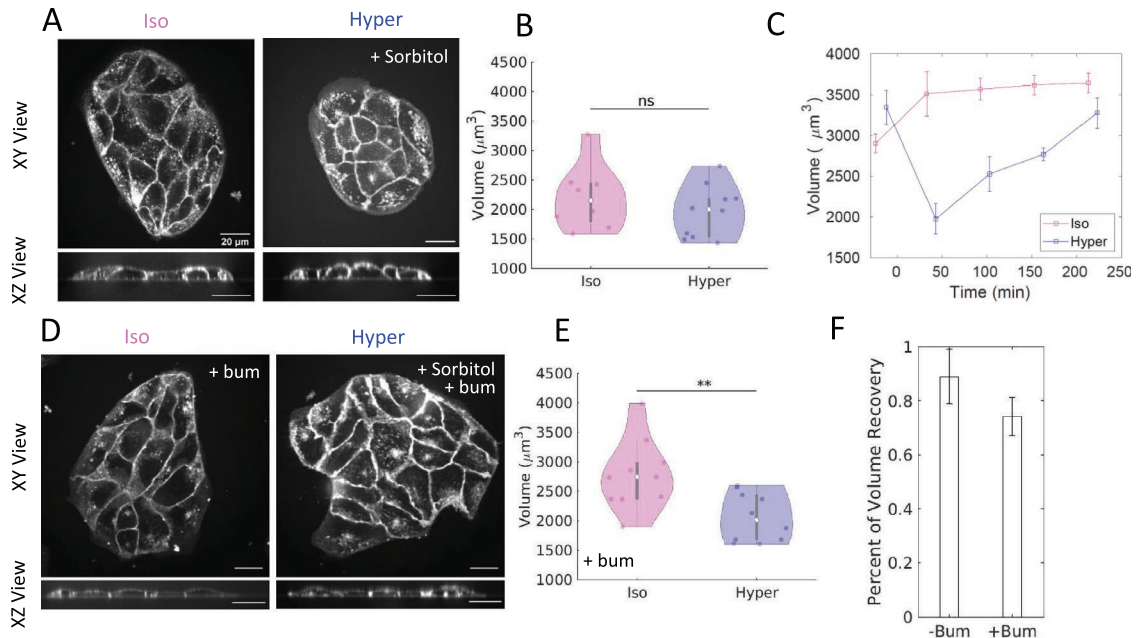


FIGURE 1: Cell volume in epithelial colonies recovers from osmotic shock via NKCC-mediated RVI. (A) Images of live MDCK-II colonies 3 h after an osmotic shock in both a top-down (XY) view and a side view (XZ). Cell membrane stained with CellMask Orange. Colonies in isotonic (Iso) conditions are in control media, while colonies under hypertonic (Hyper) conditions have 200 μM sorbitol added. Scale bars are 20 μm . (B) Violin plot of average colony cell volume in isotonic ($n = 8$ colonies) and hypertonic ($n = 10$ colonies) conditions measured 3 h after medium exchange. Colonies are 4–37 cells in size. ns = $p > 0.05$ as calculated by Student's t test. (C) Average colony cell volume under isotonic (Iso) and hypertonic (Hyper) conditions imaged every hour for 4 h. Medium exchange occurs at $t = 0$ min. Error bars represent standard error of the mean. (D) Images of live MDCK colonies 3 h after an osmotic shock and the addition of 10 μM bumetanide. Cell membrane stained with CellMask Orange. Colonies under isotonic (Iso) conditions are in control media, while colonies under hypertonic (Hyper) conditions have 200 μM sorbitol added. Scale bars are 20 μm . (E) Violin plot of average colony cell volume under isotonic (Iso) and hypertonic (Hyper) conditions measured 3 h after medium exchange and the addition of 10 μM bumetanide. $n = 10$ colonies each with 5–37 cells. ** = $p < 0.01$ as calculated by Student's t test. (F) Percent of volume recovery for colonies with and without the addition of 10 μM bumetanide. Volume recovery is measured by the ratio of mean hypertonic volume to mean isotonic volume 3 h following media exchange. Error bars represent standard error of the mean.

From comparison of these data, hyperosmotic shock leads to 20–35% cell volume reduction in both confluent monolayers plated on glass and MDCK acini grown in collagen gel. This volume reduction is not seen in MDCK colonies, which recover to 90% of their isotonic volume within 3 h (Figure 3F). This allows us to conclude that the NKCC-mediated RVI after hyperosmotic shock that preserves volume homeostasis in single cells and small colonies is hampered in confluent renal epithelial tissue.

Tight junctions are needed to prevent volume recovery in mature epithelial tissue

We speculated that the differences in volume regulation between small colonies and mature epithelium might arise from tight junctions. Tight junctions, which are critical for barrier function, are not observed in small colonies and assemble in ROCK- and ZO-1-mediated processes in confluent and polarized epithelium (Hirase *et al.*, 2001; Walsh *et al.*, 2001; Odenwald *et al.*, 2018). To assess this, we first formed monolayers and acini from MDCK-II cells with the tight junction proteins ZO-1 and ZO-2 knocked-down (Choi *et al.*, 2016). Interestingly, we found that that cell volume recovered after hyperosmotic shock in these cells. Similarly to that observed for small colonies, the volume of ZO-1-/ZO-2-deficient cells in mature epithelium decreased acutely but recovered over the subsequent several hours (Figure 4, A and B). After 3 h, the average cell volume is not significantly different than that in isotonic medium (Figure 4C). Thus,

ZO-1 is critical to the differing volume regulation observed in confluent epithelial tissue.

Another means to alter tight junction assembly is through inhibition of ROCK activity (Hirase *et al.*, 2001; Walsh *et al.*, 2001) with the addition of 25 μM of the ROCK inhibitor Y-27632 during monolayer formation. We find that ROCK inhibition also recovered the process of RVI of cells within confluent monolayers or acini that are subjected to hyperosmotic shock (Figure 5, A–E) Taken together, these data show that ROCK inhibition facilitates an 88% volume recovery in monolayers, and 94% in acini (Figure 5F). We are able to conclude that functional tight junctions are critical for the different response to hyperosmotic shock in mature epithelium than in isolated cells.

DISCUSSION

The mechanics regulating cell volume homeostasis are vital to the proper functioning of epithelial tissue in animals. We find that small colonies of renal epithelial tissue maintain their volume homeostasis and undergo NKCC-dependent RVI in a manner consistent with the pump-leakage model found in many types of individual cells. Here we find this is not the case for mature epithelium. Following a long-term hyperosmotic shock, the volume of individual cells within mature epithelium is permanently decreased (Figure 6A). Thus, RVI that allows cell volume homeostasis in response to hyperosmotic stress does not occur in mature monolayers. This lack of RVI is dependent on the tight junction assembly. Thus, we report an important role of

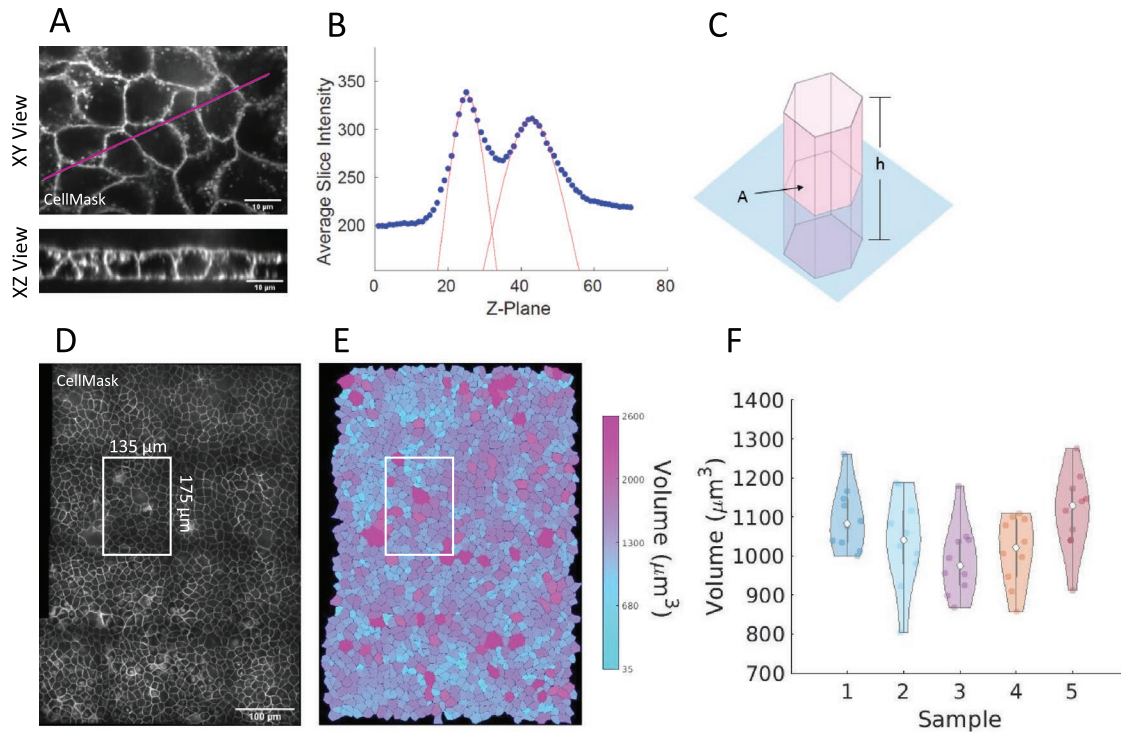


FIGURE 2: Characterizing monolayer volume and volume variation. (A) Images of live MDCK monolayers. Cell membrane stained with CellMask Orange. Scale bars are 10 μm . (B) Intensity of CellMask Orange membrane stain at different slices of the three-dimensional image, used to measure average monolayer cell height. (C) Average monolayer volume is approximated as average height, h , multiplied by average cross-sectional area, A . (D) A wide-field view of a monolayer of MDCK cells compared with the $135 \times 175 \mu\text{m}^2$ field of view used as a sample unit when measuring local volume in a monolayer. (E) The volume of each individual cell in the wide-field monolayer. (F) Violin plot representing the variation in volume across monolayers. Each sample represents a difference monolayer with each data point representing a different $135 \times 175 \mu\text{m}^2$ field of view in that monolayer.

the tight junctions in assisting cell volume regulation in epithelial tissue. Importantly, a relationship between the tight junctions and the NKCC family of ion channels has been previously reported. Results from Koumangoye *et al.* (2018) show that when NKCC1 is modified in MDCK cells, ZO-1 no longer localizes to the apical junction, instead distributing along lateral epithelial junctions. These results also indicate that the positioning of NKCC1 ion channels with respect to the osmotic pressure is not the primary driver of this response. We know that NKCC1 localizes basolaterally in MDCK-II tissue (Mykoniatis *et al.*, 2010; Koumangoye *et al.*, 2018) and so we would expect these ion channels to be sequestered away from regions of high osmotic pressure in our monolayer samples and exposed to regions of high osmotic pressure in our acini samples. Because we see similar volume recovery in both samples, we can conclude that the specific tissue membrane, either apical or basal, exposed to osmotic stress is not a significant concern for epithelial volume regulation.

Here, we surmise two possible explanations for how the tight junctions may be playing this regulatory role in epithelial tissue. One involves the tight junction as an osmotic sensor, able to communicate hydrostatic pressure across the barrier to the cytoskeleton, while the other considers the osmotic barrier created by the tight junction and how it affects osmotic pressure across epithelial tissue.

It has previously been hypothesized that the tight junction acts directly in mechanotransduction of osmolarity gradients and regulation of cell volume (Tokuda and Yu, 2019). Osmotic stress locally impacts stress at the tight junction and via action on mechano-

sensitive cytoskeleton may impact the activity of ion channels regulating RVI (Figure 6B). Without functioning tight junctions, subconfluent or inhibited tissue may lose its ability to detect the osmotic pressure gradient due to the hypertonic conditions, as an immature or disrupted tight junctional structure would cause increased paracellular transport and the absence of any shear stress between the apical and basal surfaces of the tissue, resulting in the downstream effect of active NKCC ion channels facilitating RVI. In contrast, fully confluent and uninhibited epithelial monolayers sense this stress at their “leak-proof” tight junctions, and this results in the suppression of volume homeostasis through as yet unknown intercellular signaling. This model is supported by evidence that hydrostatic pressure on the tight junction affects both the localization of the tight junction protein claudin-1, which instead disperses to the cytoplasm, and lateral actin structure (Tokuda *et al.*, 2009), meaning that stress on the tight junction causes tangible changes to the actin cytoskeleton. In turn, the actin cytoskeleton has been shown to regulate and organize variety of ion channels and related transporters associated with volume regulation (Papakonstanti *et al.*, 2000; Maz-zochi *et al.*, 2006). Specifically, in airway epithelial tissue, actin stabilization has been found to activate NKCC1 channels through the serine–threonine protein kinase PKC- δ (Liedtke *et al.*, 2003).

An equally interesting explanation is that an intact tight junction serves to confine the osmotic pressure to only a small subsection of the epithelial membrane (Figure 6C). Instead of an epithelial cell being surrounded by hyperosmotic pressure at all membranes, as we see when examining single-cell volume regulation, the tight junction restricts that osmotic pressure to only one side of the

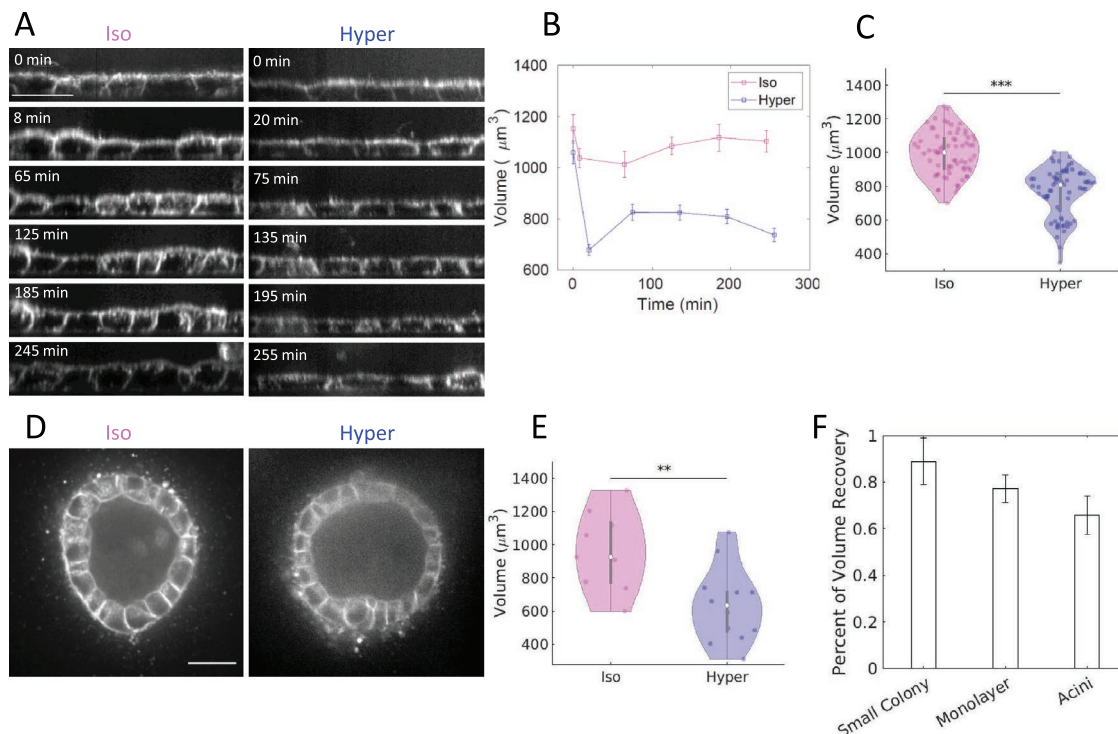


FIGURE 3: Mature epithelial tissue does not recover from a long-term osmotic shock. (A) Images of live XZ views of MDCK monolayers taken over 5 h. Cell membrane stained with CellMask Orange. Monolayers under isotonic (Iso) conditions are in control media, while those under hypertonic (Hyper) conditions have 200 μM sorbitol added. Scale bars are 20 μm . (B) Average cell volume under isotonic (Iso) and hypertonic (Hyper) conditions imaged every hour for 4 h. Medium exchange occurs at $t = 0$ min. Error bars represent standard error of the mean. $n = 10$ fields of view from one monolayer. (C) Violin plot of average monolayer cell volume under isotonic and hypertonic conditions measured 3 h after medium exchange. $n = 70$ fields of view across seven separate monolayers of varying density with 100–165 cells per field of view. $*** = p < 0.0001$ as calculated by Student's t test. (D) Cross-sections of hollow MDCK acini grown in collagen gel. Cell membrane stained with CellMask Orange. Acini under isotonic (Iso) conditions are in control medium, while those under hypertonic (Hyper) conditions have 200 μM sorbitol added. Scale bars are 20 μm . (E) Violin plot of average acini cell volume under isotonic ($n = 9$ acini) and hypertonic ($n = 13$ acini) conditions measured 3 h after medium exchange. $** = p < 0.01$ as calculated by Student's t test. (F) Volume recovery is measured by the ratio of mean hypertonic volume to mean isotonic volume 3 h following medium exchange. Error bars represent standard error of the mean.

epithelial tissue and impacts RVI. This hypothesized mechanism poses that geometrically constrained osmotic stress across the apical/basal surfaces of the tissue affects cellular volume regulation differently than osmotic stress across the cellular membrane. In our results, mature monolayers with functional tight junctions are only exposed to hyperosmotic pressure at the apical membrane and acini are only exposed at the basolateral membrane. Thus, our data do not indicate that the geometry of the osmotic shock is important for this response, as one might expect given known localization of the NKCC1 channel to the basolateral surface (Mykoniatis *et al.*, 2010; Koumangoye *et al.*, 2018). Instead, they suggest that cells react differently to osmotic pressure gradients across the apical-basal plane than to those across the cell membrane.

Future work is required to understand the mechanisms controlling of volume regulation in mature epithelium, including how tight junctions impact NKCC ion channel activity. The details of the relationship between NKCC activity and tight junctions have been linked to dysfunction and inflammation in both the gut (Koumangoye *et al.*, 2020) and the brain (Wang *et al.*, 2022), where activating NKCC1-related pathways was found to disrupt the tight junctions of the blood-brain barrier. We are able thus to conclude that tight junctions in mature epithelium suppress volume homeostasis, and cell volume regulation in epithelial tissue is qualitatively different from that of

single cells. Given the known consequences of cell volume regulation for cellular physiology, these results have significant consequences for control of mechanotransduction pathways in epithelial tissue.

MATERIALS AND METHODS

[Request a protocol](#) through *Bio-protocol*.

Cell culture

MDCK-II cells were cultured in DMEM and supplemented with 10% fetal bovine serum (FBS; ThermoFisher Scientific), 2 mM L-glutamine (Invitrogen), and penicillin–streptomycin (Invitrogen). Cells were incubated in a humidified environment at 37°C and 5% CO_2 . MDCK ZO-1/ZO-2 KD cells were generously provided by Mark Peifer (University of North Carolina).

Osmotic shock treatment

Hyperosmotic medium was created through the addition of 200 mOsm of sorbitol (Phytotechnology Laboratories) to 290 mOsm DMEM medium to make 490 mOsm hypertonic medium.

Sample creation

To create small colonies, MDCK cells were plated sparsely to coat the glass bottom of a four-well chamber (Ibidi) and incubated for

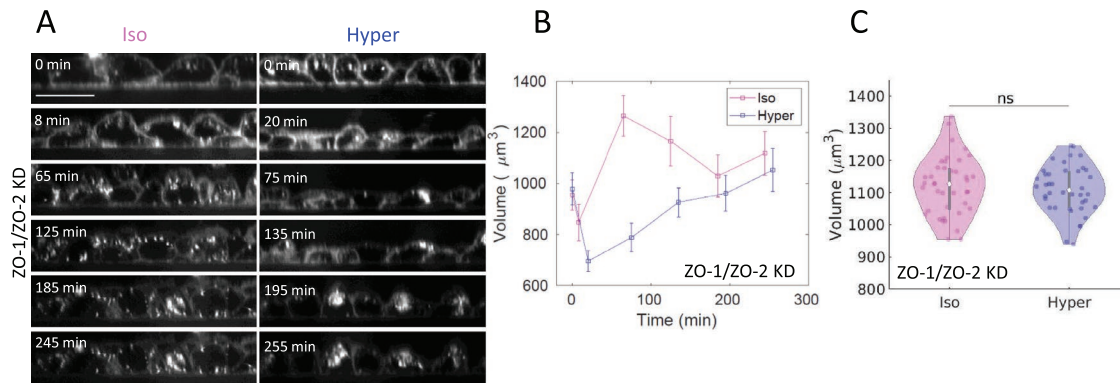


FIGURE 4: The tight junction protein ZO-1 is required to prevent volume recovery in mature epithelial tissue. (A) Images of live XZ views of ZO-1/ZO-2 knock-down (KD) MDCK monolayers taken over 5 h. Cell membrane stained with CellMask Orange. Monolayers under isotonic (Iso) conditions are in control medium, while those under hypertonic (Hyper) conditions have 200 μM sorbitol added. Scale bars are 20 μm . (B) Average cell volume of ZO-1/ZO-2 KD monolayers under isotonic (Iso) and hypertonic (Hyper) conditions imaged every hour for 5 h. Medium exchange occurs at $t = 0$ min. Error bars represent standard error of the mean. $n = 10$ fields of view in one monolayer. (C) Violin plot of average ZO-1/ZO-2 KD monolayer cell volume under isotonic and hypertonic conditions measured 3 h after media exchange. $n = 40$ fields of view across four separate monolayers of varying density with 99–150 cells per field of view. $ns = p > 0.05$ as calculated by Student's t test.

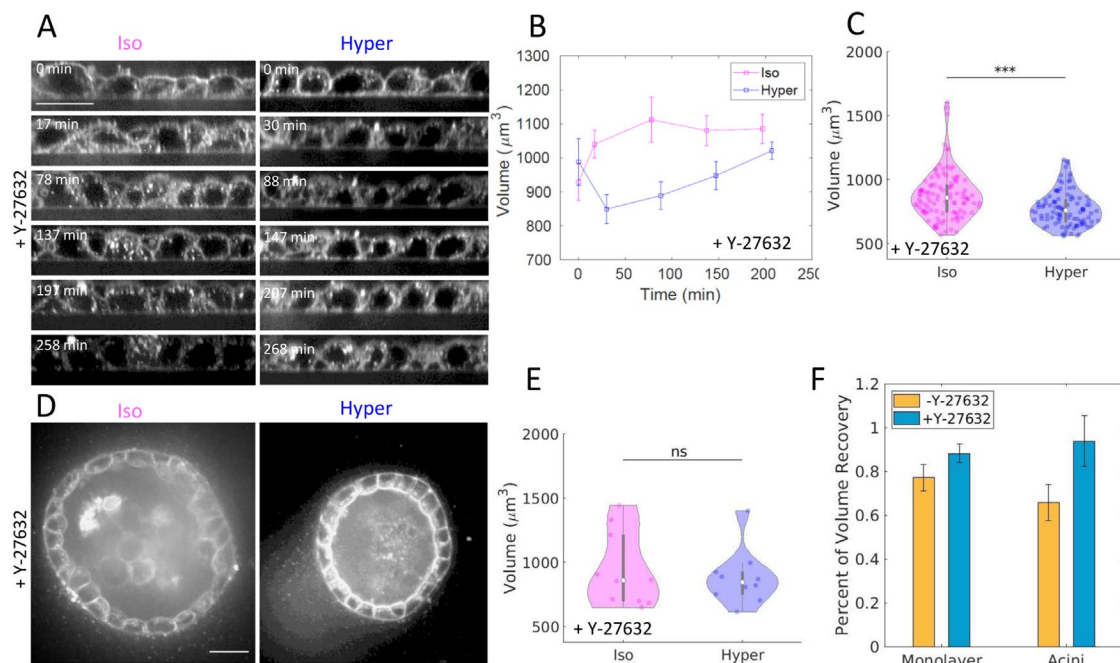


FIGURE 5: ROCK is needed to prevent volume recovery in mature epithelial tissue. (A) Images of live XZ views of MDCK monolayers with 25 μM of the ROCK inhibitor Y-27632 taken over 4 h. Cell membrane stained with CellMask Orange. Monolayers under isotonic (Iso) conditions are in control medium, while those under hypertonic (Hyper) conditions have 200 μM sorbitol added. Scale bar is 20 μm . (B) Average cell volume of monolayers with 25 μM Y-27632 under isotonic and hypertonic conditions imaged every hour for 4 h. Medium exchange occurs at $t = 0$ min. Error bars represent standard error of the mean. $n = 10$ fields of view in one monolayer. (C) Violin plot of average monolayer cell volume with 25 μM Y-27632 under isotonic and hypertonic conditions measured 3 h after medium exchange. $n = 110$ fields of view across 11 separate monolayers of varying density with 40–160 cells per field of view. $*** = p < 0.0001$ as calculated by Student's t test. (D) Cross-sections of hollow MDCK acini grown in collagen gel, with 25 μM Y-27632 added 3 h before imaging. Cell membrane stained with CellMask Orange. Acini under isotonic (Iso) conditions are in control medium, while those under hypertonic (Hyper) conditions have 200 μM sorbitol added. Scale bars are 20 μm . (E) Violin plot of average acini cell volume under isotonic ($n = 10$ acini) and hypertonic ($n = 10$ acini) conditions measured 3 h after medium exchange. $ns = p > 0.05$ as calculated by Student's t test. (F) Volume recovery is measured by the ratio of mean hypertonic volume to mean isotonic volume 3 h following medium exchange. Error bars represent standard error of the mean.

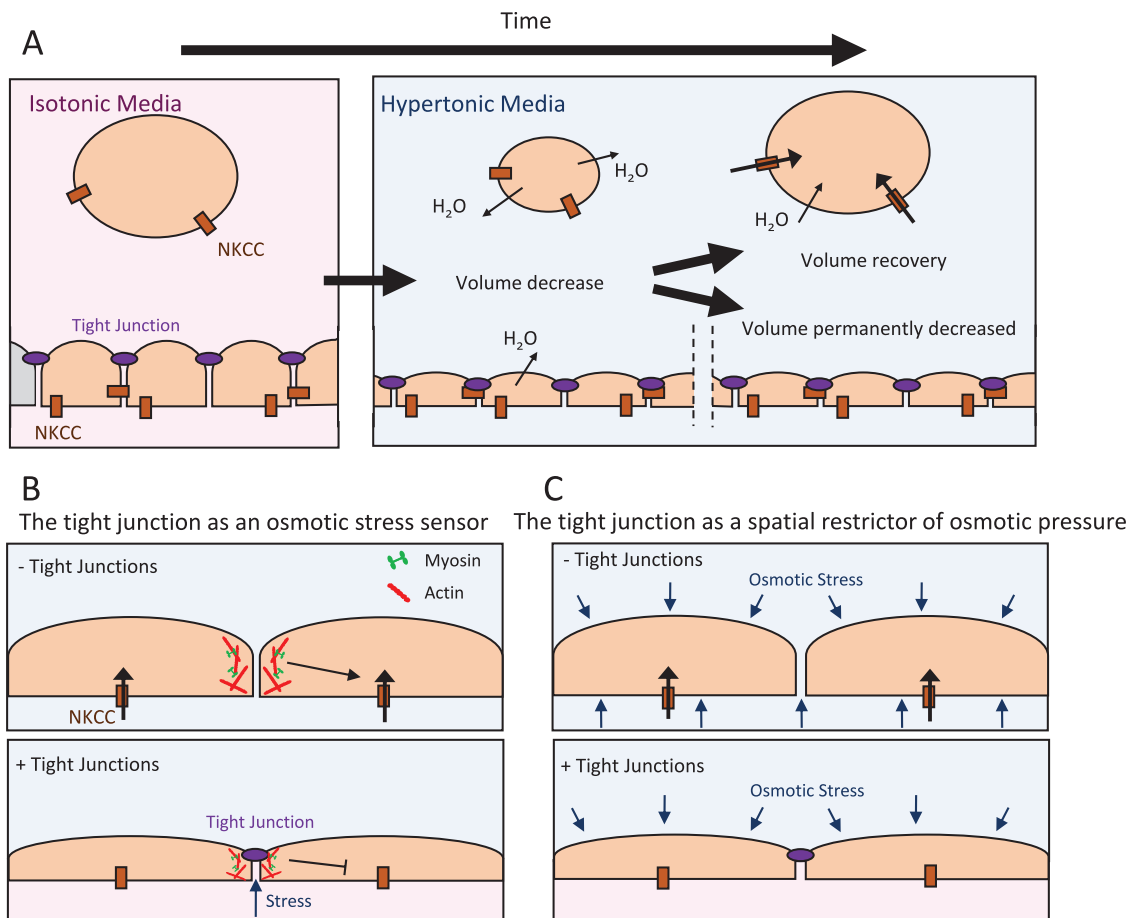


FIGURE 6: Tight junction regulation of volume homeostasis. (A) A schematic depicting the dynamics of volume homeostasis in single cells and in mature epithelial tissue. With the addition of hyperosmotic medium, single cells first shrink in volume as water exits the cell to the surrounding media. Over time, NKCC ion channels pump ions back into the cells, allowing water to follow the osmotic gradient and restore the cell's volume. A mature epithelium exposed to hypertonic medium also decreases in volume as water exits into the surrounding medium. However, the NKCC ion pumps are inactive and no RVI occurs. (B) A schematic of the potential role the tight junction plays as an osmotic stress sensor. In the case of epithelium with permeable, that is, leaky, tight junctions (Upper), the absence of the tight junction allows volume homeostasis to occur through NKCC ion channels. In confluent tissue with functioning tight junctions (Lower), the stress across the tight junction is transmitted to the mechanosensitive actomyosin cytoskeleton. This results in the inhibition of volume homeostasis, and cell volume does not recover. (C) A schematic of the possible role the tight junction plays as a spatial restrictor of osmotic stress. In this model, epithelia with permeable tight junctions (Upper) have zero osmotic gradient across the epithelium, and thus are surrounded at all membranes by hyperosmotic stresses, promoting RVI reminiscent of single-cell volume homeostasis. In contrast, epithelia with impermeable tight junctions (Lower) create a barrier preventing hyperosmotic medium from reaching across to both sides of the epithelia, creating a nonzero osmotic gradient and spatially restricting where osmotic pressure is applied to the cells in the epithelium.

24 h. To create a mature monolayer, MDCK cells were plated densely to coat the glass bottom of a four-well (for time-lapse imaging) or eight-well (for non-time-lapse imaging) chamber (Ibidi). The cells were then incubated for 48 h with a change of medium at 24 h. Acini were formed by sparsely plating MDCK cells in 2 mg/ml collagen gel for 8 d with the addition of serum starved (1% FBS) DMEM changed every 48 h. Inhibitors and osmotic treatments were added 3 h before imaging. ROCK inhibited cells were treated with 25 μ M Y-27632 (Sigma) 3 h before live imaging. NKCC-inhibited cells were treated with 10 μ M bumetanide (Sigma) 3 h before live imaging.

Microscopy and live cell imaging

CellMask Orange (2 μ l/ml; Invitrogen) was added to samples 30 min before imaging to stain the cell membrane. Samples were imaged on an inverted T-E microscope (Nikon) with a confocal CSU-X spin-

ning disk (Yokogawa Electric Corporation), a stage controller (Prior), and a CMOS camera (Zyla-Andor). Metamorph software was used to control the microscope and collect images. A stage incubator (Chamlide and Quorum Technologies) with CO₂, humidity, and temperature control was used for time-lapse experiments, while a stage heater (Nevtek, ASI 400) was used for non-time-lapse experiments. A 561-nm laser (MPB Communications, VFL-P Series) was used to illuminate the CellMask Orange stain. Images were acquired using a 60 \times Plan Apo NA water immersion objective with a NA of 1.20 and a WD of 0.31–0.28 (Nikon). Three-dimensional images were collected using z-stacks of 0.25 μ m steps.

Height and volume analysis

Both ImageJ and Matlab were used for image analysis of monolayer height and volume. Average monolayer height (excluding ZO1/ZO2

KD monolayers) was measured using Matlab by taking the average image intensity for each z-stack of the three-dimensional image. The peaks in average image intensity at the apical and basal membranes from the CellMask Orange dye were fitted to a Gaussian and the distance between these peaks was measured to find the monolayer height. In ImageJ, the Cell Counter tool was used to determine the density of cells in each sample image. This density measurement was used to determine the average cross-sectional area of the cells in the image. The average volume of cells in the monolayer was found by multiplying the average cross-sectional area by the average monolayer height. Volume measurements for ZO-1/ZO-2 KD monolayers, as well as all colonies and acini, were found using an alternate method. For ZO-1/ZO-2 KD cells and colonies this was because their extended apical domain is not well characterized by the assumption that the apical membrane is flat, and for acini it was because the cells were not grown on a flat surface. In these cases, average cell volume was found by measuring cell junction height, maximum cell height, and basal area for sample cells. This allowed us to model the volume of the cell as a cylinder that is the height of the cell junction length plus a hemisphere on top.

Violin Plots

The width of each colored region represents volume kernel density, which is an estimate of the probability density function of the average cell volume. The white point represents the median cell volume for all colonies measured, and the gray bar represents the interquartile range, meaning the middle 50% of the volume range.

Quantification and Statistical analysis

Image analysis and quantification were performed in Fiji, Excel, and Matlab. Matlab was used to perform statistical analysis and calculate statistical significance using two-tailed Student *t* tests where *ns* = *p* > 0.05, * = *p* < 0.05, ** = *p* < 0.01, and *** = *p* < 0.0001.

ACKNOWLEDGMENTS

This work was supported by funding from NIH RO1 GM104032 and ARO MURI W911NF1410403. We are grateful to Mark Peifer (UNC Chapel Hill) for the ZO-1/ZO-2 KD MDCK cell line, and to Jeffrey Matthews, Eric Delpire, and Patrice Bouyer for valuable discussions.

REFERENCES

Beck FX, Burger-Kentscher A, Müller E (1998). Cellular response to osmotic stress in the renal medulla. *Pflugers Arch* 436, 814–827.

Carmosino M, Giménez I, Caplan M, Forbush B (2008). Exon loss accounts for differential sorting of Na-K-Cl cotransporters in polarized epithelial cells. *Mol Biol Cell* 19, 4341–4351.

Choi W, Acharya BR, Peyret G, Fardin M-A, Mège R-M, Ladoux B, Yap AS, Fanning AS, Peifer M (2016). Remodeling the zonula adherens in response to tension and the role of afadin in this response. *J Cell Biol* 213, 243–260.

Delpire E, Gagnon KB (2018). Water homeostasis and cell volume maintenance and regulation. In: *Current Topics in Membranes*, Elsevier, 3–52.

Finan JD, Guilak F (2010). The effects of osmotic stress on the structure and function of the cell nucleus. *J Cell Biochem* 109, 460–467.

Fischbarg J (2010). Fluid transport across leaky epithelia: central role of the tight junction and supporting role of aquaporins. *Physiol Rev* 90, 1271–1290.

Günzel D, Yu ASL (2013). Claudins and the modulation of tight junction permeability. *Physiol Rev* 93, 525–569.

Haas M (1994). The Na-K-Cl cotransporters. *Am J Physiol Cell Physiol* 267, C869–C885.

Hirase T, Kawashima S, Wong EYM, Ueyama T, Rikitake Y, Tsukita S, Yokoyama M, Staddon JM (2001). Regulation of tight junction permeability and occludin phosphorylation by RhoA-p160ROCK-dependent and -independent mechanisms. *J Biol Chem* 276, 10423–10431.

Hoffmann EK, Lambert IH, Pedersen SF (2009). Physiology of cell volume regulation in vertebrates. *Physiol Rev* 89, 193–277.

Koumangoye R, Omer S, Delpire E (2018). Mistargeting of a truncated Na-K-2Cl cotransporter in epithelial cells. *Am J Physiol Cell Physiol* 315, C258–C276.

Koumangoye R, Omer S, Kabeer MH, Delpire E (2020). Novel human NKCC1 mutations cause defects in goblet cell mucus secretion and chronic inflammation. *Cell Mol Gastroenterol Hepatol* 9, 239–255.

Lee B, Moon KM, Kim CY (2018). Tight junction in the intestinal epithelium: its association with diseases and regulation by phytochemicals. *J Immunol Res* 2018, 1–11.

Lee DBN, Huang E, Ward HJ (2006). Tight junction biology and kidney dysfunction. *Am J Physiol-Ren Physiol* 290, F20–F34.

Liedtke CM, Hubbard M, Wang X (2003). Stability of actin cytoskeleton and PKC- δ binding to actin regulate NKCC1 function in airway epithelial cells. *Am J Physiol-Cell Physiol* 284, C487–C496.

Liu W-Y, Wang Z-B, Zhang L-C, Wei X, Li L (2012). Tight junction in blood-brain barrier: an overview of structure, regulation, and regulator substances. *CNS Neurosci Ther* 18, 609–615.

Mazzochi C, Benos DJ, Smith PR (2006). Interaction of epithelial ion channels with the actin-based cytoskeleton. *Am J Physiol Renal Physiol* 291, F1113–F1122.

Mykoniatis A, Shen L, Fedor-Chaiken M, Tang J, Tang X, Worrell RT, Delpire E, Turner JR, Matlin KS, Bouyer P, et al. (2010). Phorbol 12-myristate 13-acetate-induced endocytosis of the Na-K-2Cl cotransporter in MDCK cells is associated with a clathrin-dependent pathway. *Am J Physiol-Cell Physiol* 298, C85–C97.

Odenwald MA, Choi W, Kuo W-T, Singh G, Sailer A, Wang Y, Shen L, Fanning AS, Turner JR (2018). The scaffolding protein ZO-1 coordinates actomyosin and epithelial apical specializations in vitro and in vivo. *J Biol Chem* 293, 17317–17335.

Papakonstanti EA, Vardaki EA, Stournaras C (2000). Actin cytoskeleton: a signaling sensor in cell volume regulation. *Cell Physiol Biochem* 10, 257–264.

Strange K (1993). *Cellular and Molecular Physiology of Cell Volume Regulation*, CRC Press.

Tokuda S, Miyazaki H, Nakajima K, Yamada T, Marunaka Y (2009). Hydrostatic pressure regulates tight junctions, actin cytoskeleton and transcellular ion transport. *Biochem Biophys Res Commun* 390, 1315–1321.

Tokuda S, Yu ASL (2019). Regulation of epithelial cell functions by the osmolality and hydrostatic pressure gradients: a possible role of the tight junction as a sensor. *Int J Mol Sci* 20, 3513.

Varadarajan S, Stephenson RE, Misterovich ER, Wu JL, Erofeev IS, Goryachev AB, Miller AL (2021). Mechanosensitive calcium signaling in response to cell shape changes promotes epithelial tight junction remodeling by activating RhoA. 2021.05.18.444663.

Walsh SV, Hopkins AM, Chen J, Narumiya S, Parkos CA, Nusrat A (2001). Rho kinase regulates tight junction function and is necessary for tight junction assembly in polarized intestinal epithelia. *Gastroenterology* 121, 566–579.

Wang J, Liu R, Hasan MN, Fischer S, Chen Y, Como M, Fiesler VM, Bhuiyan MIH, Dong S, Li E, et al. (2022). Role of SPAK–NKCC1 signaling cascade in the choroid plexus blood–CSF barrier damage after stroke. *J Neuroinflammation* 19, 91.

Zehnder SM, Suaris M, Bellaire MM, Angelini TE (2015). Cell volume fluctuations in MDCK monolayers. *Biophys J* 108, 247–250.